Boundary-Layer Theory for Pressure and Drag of a Wavy Surface

Kenneth H. Rogers*
Northrop Corporation, Newbury Park, Calif.

The approximate theory presented, including the effect of the boundary layer, permits a much more accurate determination of pressure and drag of wavy surfaces in subsonic and supersonic flow (for $M < 2.0$) than is possible with inviscid flow theory. The B.L. (boundary layer) theory shows that the effective wave height and associated pressure decrease and eventually approach zero as the ratio of boundary-layer thickness to wave length increases. In supersonic flow, the decrease in effective wave height due to the boundary layer is accompanied by an aft phase shift in the B.L. wave, further decreasing the pressure drag due to the surface waves. The analysis correlates the theory with the results of surface waviness experiments conducted at the Langley Research Center and includes an estimate of drag contribution due to Görtler vortices generated by multiple waves. Application of the theory to a subsonic wing shows that surface waviness of appreciably smaller magnitude than that commonly found on military aircraft causes a significant detrimental effect on the drag-rise characteristics. Additional experimental research is needed to better evaluate the phase shift in supersonic flow, and the effect of Görtler vortices in both subsonic and supersonic flow.

Nomenclature

B.L. = boundary layer
c = velocity of sound
C = wing chord
C_D = drag coefficient, D/qs
$C(D_P)$ = pressure-drag coefficient
C_f = surface friction coefficient, D/qs
C_p = pressure coefficient, P/q
D = drag
H = boundary-layer parameter δ^*/Θ
l = length of the wave
M = Mach number at the outer edge of the boundary layer
P = pressure
P_t = total pressure
q = dynamic pressure
R = Reynolds number; for example, $R_C = \rho UC/\mu$
R' = Reynolds number per ft
S = reference area
u = velocity within the boundary layer
U = velocity at the outer edge of the boundary layer
x = distance in the flow direction
y = distance normal to the surface and flow
β = compressibility factor $|1 - M^2|^{.5}$
Δ = a variation or increment of a parameter; e.g., ΔC_p
δ = total thickness of the boundary layer
δ^* = displacement thickness of the boundary layer
$\delta^* = \int_0^\delta (1 - (\rho u/\rho_0 U))\, dy$
ϵ_w = one-half the height of surface waves (subscript "w" refers to "wall")
ϵ = effective half-height of the waves
θ = momentum thickness of the boundary layer
$\theta = \int_0 (\rho u/\rho_0 U)\,(1 - (u/U))\, dy$
θ_x = angular distance along wave (in the direction of flow)
μ = coefficient of viscosity
ρ = density
τ = thickness ratio of wing
ϕ = phase shift of the wave at the outer edge of the boundary layer

Subscripts
i = inviscid flow
o = outer edge of boundary layer

Received February 20, 1973; revision received March 26, 1974. The author wishes to express his appreciation to the reviewers, who supplied a number of suggestions resulting in improvements in this paper.

Index categories: Aircraft Aerodynamics (Including Component Aerodynamics); Boundary Layer and Convective Heat Transfer—Turbulent; Multiphase Flows.

*Engineering Specialist, Ventura Division. Member AIAA.

I. Introduction

THE theory of subsonic and supersonic two-dimensional inviscid flow over a wavy wall was first presented by Ackeret in the period 1925 to 1928[1,2] and is now a familiar part of modern textbooks in gasdynamics (Ref. 3, for example). The theory is an application of the small perturbation theory presented in lectures by Prandl several years prior to 1925. However, at Mach numbers less than approximately 2.0, the inviscid flow theory does not predict the pressure and drag of surface waves in real flow with sufficient accuracy for practical application. In typical experiments simulating aircraft flight near the transonic region, the measured values of pressure and drag of a wavy surface can be less than half the values calculated from the inviscid flow theory.[4-6] The discrepancy between experiment and theory generally is attributed to B.L. (boundary-layer) effects, but so far, no one has published a B.L. theory correlating experiment and theory for this particular problem.

The purpose of this paper is to include B.L. effects in the subsonic and supersonic theories for inviscid flow just described so that the results are of practical use in aerodynamic analyses. The new theory primarily deals with a "effective" waviness, which is a modification of the wall waviness, due to variation in B.L. displacement thickness.

In the case of repeated waves, Görtler vortices may be generated in the unstable B.L. flow in the concave region of the waves. If the B.L. instability is strong enough to form the Görtler vortices the increased surface friction and increased B.L. thickness due to the Görtler vortices should be included in the analysis. The evaluations of the effects of Görtler vortices, as presented here, necessarily are approximations because of the scarcity of published research data on the subject.

The determination of the pressure and drag due to surface waviness is of practical as well as academic interest. Experiments at the NASA Langley Research Center have shown that surface waviness of a magnitude commonly found on transonic aircraft can provide a significant contribution to the total drag of the aircraft. The problem

can be avoided, technically, by building aircraft with negligible surface waviness, but the manufacturing cost increases. Thus, it is important to be able to accurately assess the flight performance penalty associated with surface waviness. The problem may be even more important for the smaller aerial RCVs (remotely controlled vehicles) than for manned aircraft because a given surface wave configuration in transonic and supersonic flow produces more pressure drag in the thinner boundary layer of the smaller vehicle.

II. Subsonic Theory—Pressure Coefficient

The pressure coefficient for subsonic inviscid flow over a wavy surface, according to the small perturbation theory of Chap. 8, Ref. 3, is:

$$\Delta C_{p_i} = (4\pi\epsilon_w/\beta l)\sin(2\pi x/l) \tag{1}$$

where ΔC_p is the pressure coefficient $\Delta p/q$, ϵ_w is one-half the wave height of the wall, l is the wavelength, and β is the Prandtl-Glauert factor $(1 - M^2)^{0.5}$. The maximum pressure coefficient, from Eq. (1), is

$$\Delta C_{p_{\max_i}} = \pm\ 4\pi\epsilon_w/\beta l \tag{2}$$

In the following subsonic flow analysis, an "effective" value of the waviness ϵ is used to calculate the pressure variation, using Eq. (2). The effective value of waviness used is the waviness at the outer edge of the boundary layer, which is the wall waviness ϵ_w less the variation in B.L. displacement thickness $\Delta\delta^*$.

The derivation of the theory proceeds as follows. An expression for the B.L. displacement thickness variation $\Delta\delta^*$ in terms of the forcing function ΔC_p can be derived from the momentum integral equation for compressible flow, as presented in Eq. (15.59) of Ref. 7, neglecting the effect of the wall friction perturbation on an already existent boundary layer

$$\Delta\delta^*/\delta^* = \Delta\theta/\theta = -(\Delta U/U)(2 + H - M^2) \tag{3}$$

where θ is the momentum thickness of the boundary layer, U is the local external velocity, H is the shape factor δ^*/θ, and M is the local Mach number at the edge of the boundary layer.

It is assumed in Eq. (3) that the perturbation in skin friction due to wall waviness is small compared with the perturbation in B.L. thickness. Also

$$\Delta U/U = -\Delta C_p/2 \tag{4}$$

from Eqs. (8-12) of Ref. 3. Substituting Eq. (4) into Eq. (3)

$$\Delta\delta^* = \delta^*(2 + H - M^2)\,\Delta C_p/2 \tag{5}$$

Equation (5) shows that the variation $\Delta\delta^*$ is proportional to and in phase with the pressure coefficient ΔC_p. Figure 1 shows the relationship of the pressure wave, B.L. wave and wall wave, and shows how the B.L. wave is reduced in amplitude by the variation in B.L. displacement thickness. Equation (2) now can be rewritten for real flow in terms of the effective value ϵ as follows:

$$\Delta C_{p_{\max}} = \pm\frac{4\pi\epsilon}{\beta l} = \pm\frac{4\pi(\epsilon_w - |\Delta\delta^*_{\max}|)}{\beta l}$$

or

$$\Delta C_{p_{\max}} = \pm\frac{4\pi[\epsilon_w - \delta^*(2 + H - M^2)\Delta C_{p_{\max}}/2]}{} \tag{6}$$

where ϵ is the half-height of the B.L. wave. Solving Eq. (6) for $\Delta C(p_{\max})$

$$\Delta C_{p_{\max}} = \pm\,(4\pi\epsilon_w/\beta l)\Big/\left[1 + \frac{2\pi}{\beta}(2 + H - M^2)\frac{\delta^*}{l}\right] \tag{7}$$

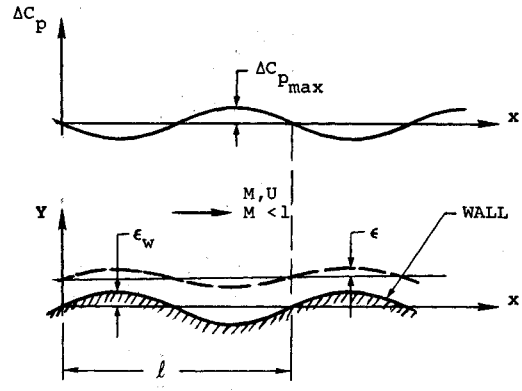

Fig. 1 Surface wave and pressure wave in subsonic flow.

Examples of $\Delta C(p_{\max})$ vs M are shown in Sec. V, correlation of experiment and theory.

The pressure coefficient ratio, the ratio of pressure coefficients for real and inviscid flow, is

$$\frac{C_{p_{\max}}}{C_{p_{\max_i}}} = (1 - \Delta\delta^*_{\max}/\epsilon_w) = \left\{1\Big/\left[1 + (2 + H - M^2)\frac{2\pi}{\beta}\left(\frac{\delta^*}{l}\right)\right]\right\} \tag{8}$$

Equation (8) shows that the pressure coefficient ratio approaches zero as the B.L. thickness parameter δ^*/l increases.

III. Supersonic Theory

A. Pressure Coefficient and Phase Shift

The pressure coefficient for supersonic inviscid flow over a wavy surface, according to the small-perturbation theory of Chap. 8, Ref. 3, is

$$\Delta C_{p_i} = -(4\pi\epsilon_w/\beta l)\cos(2\pi x/l) \tag{9}$$

Equation (9) is similar to Eq. (1) for subsonic flow except that the cosine rather than sine function indicates a phase shift of the pressure such that the maximum values of pressure occur on the slopes rather than the peaks of the waves, and the value of the compressibility factor β is

$$\beta = (M^2 - 1)^{0.5} \tag{10}$$

The maximum value of the pressure coefficient in supersonic inviscid flow is the same equation used for inviscid subsonic flow:

$$\Delta C_{p_{\max_i}} = \pm\,4\pi\epsilon_w/\beta l \tag{11}$$

In real flow the surface wave half-height ϵ_w is assumed replaced by an effective half-height ϵ which is smaller than ϵ_w and is displaced aft by a phase angle ϕ due to the boundary layer (Fig. 2). The effective waveform assumed is that of the outer edge of the boundary layer. Expressions for the effective half-height ϵ and the phase angle ϕ are derived as follows, with reference to Fig. 2.

Assume that the maximum pressure occurs at the position of maximum slope of the B.L. wave Y_2 in accordance with supersonic flow theory. Also assume that the relationship between B.L. displacement thickness and pressure coefficient applies as shown in Eq. (5); i.e., the position of maximum pressure corresponds to the position of maximum thickness of the B.L. displacement.

In the mathematical analysis it is convenient to assume that both the B.L. wave Y_2 and the surface wave Y_1 are sine waves. The assumption that the variation in boundary-layer thickness is proportional to the pressure coefficient implies that the difference between Y_2 and Y_1 also

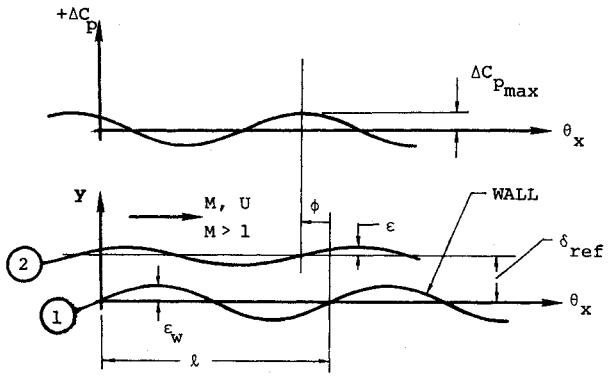

Fig. 2 Surface wave and pressure wave in supersonic flow.

is a sine wave, which is not true. However, the error is assuming that $Y_2 - Y_1$ is a sine wave is negligibly small; in a sample calculation, for a phase shift $\phi = 45°$, the maximum discrepancy is less than 1%. Since the error is very small the assumptions are considered valid for an approximate solution.

The equation for the wall is

$$Y_1 = \epsilon_w \sin\theta_x \tag{12}$$

and the equation for the B.L. wave is

$$Y_2 = \delta_{ref} + \epsilon \sin(\theta_x - \phi) \tag{13}$$

The difference is

$$\Delta y = Y_2 - Y_1 = \delta_{ref} + \epsilon \sin(\theta_x - \phi) - \epsilon_w \sin\theta_x \tag{14}$$

Assume that Δy is maximum when $\theta_x = \phi$, then

$$\cos\phi = (\epsilon/\epsilon_w) \tag{15}$$

and

$$\sin\phi = (\Delta y_{max} - \delta_{ref})/\epsilon_w \tag{16}$$

As in the subsonic analysis, assume that the variation in boundary-layer thickness ($\Delta y_{max} - \delta_{ref}$) is the variation in displacement thickness $\Delta\delta^*_{max}$; then

$$\cos\phi = \left[1 - \left(\frac{\Delta\delta^*_{max}}{\epsilon_w}\right)^2\right]^{0.5} = \frac{\epsilon}{\epsilon_w} \tag{17}$$

and

$$\sin\phi = \frac{\Delta\delta^*_{max}}{\epsilon_w} \tag{18}$$

The equation for maximum pressure coefficient is

$$\Delta C_{p_{max}} = \pm \frac{4\pi\epsilon_w}{\beta l}\left[1 - \left(\frac{\Delta\delta^*_{max}}{\epsilon_w}\right)^2\right]^{0.5} \tag{19}$$

and

$$\frac{\Delta C_{p_{max}}}{\Delta C_{p_{max_i}}} = \left[1 - \left(\frac{\Delta\delta^*_{max}}{\epsilon_w}\right)^2\right]^{0.5} = \cos\phi \tag{20}$$

Now let

$$\Delta\delta^*_{max}/\delta^* = [(2 + H - M^2)/2]\Delta C_{p_{max}} \tag{21}$$

as in subsonic flow. Substituting Eq. (21) into (20):

$$\frac{\Delta C_{p_{max}}}{\Delta C_{p_{max_i}}} = \left\{\frac{1}{1 + \left[(2 + H - M^2)\frac{2\pi}{\beta}\left(\frac{\delta^*}{l}\right)\right]^2}\right\}^{.5} = \cos\phi \tag{22}$$

Equation (22) shows that the pressure amplitude ratio $\Delta C(p_{max})/\Delta C(p_{max})$ approaches zero as the B.L. thickness ratio δ^*/l increases, as in subsonic flow, and also shows that the pressure phase-shift ϕ approaches $\pi/2$ as the ratio δ^*/l increases. Examples of $\Delta C(p_{max})$ vs Mach number for a turbulent boundary layer are presented in Sec. V.

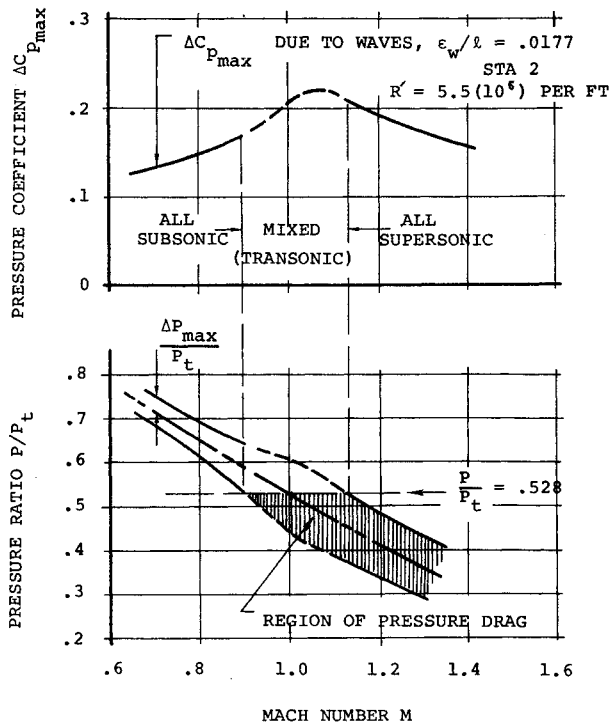

Fig. 3 Pressure diagram showing regions of subsonic and supersonic flow.

B. Pressure-Drag Coefficient

An expression for the pressure-drag coefficient $\Delta C(D_p)$ in terms of the pressure coefficient ΔC_p in supersonic flow is derived as follows:

$$\Delta C_p = (2/\beta)(dy/dx) = (2/\beta)(2\pi\epsilon/l)\cos(2\pi x/l) \tag{23}$$

and

$$\Delta C_{D_p} = (2/\beta l)(\cos\phi)\int_0^l (dy/dx)^2 dx \tag{24}$$

where ϕ is the phase-shift of the boundary-layer pressure wave.

The two preceding equations are versions of Eqs. (8.35) and (8.36), p. 214, Ref. 3, except for the factor cos ϕ. The factor cos ϕ is derived by assuming that the drag coefficient is proportional to the product of a sine wave representing pressure and a sine wave representing the slope of the surface wave. The integrated product of the two sine waves, as one wave is shifted an amount of ϕ, is proportional to cos ϕ, as shown in the following exercise.

Let slope of surface = $a \sin\theta$. Let pressure = $b \sin(\theta - \phi)$. Then

$$\text{drag} \sim ab\int_0^{2\pi} \underset{\alpha}{\sin\theta}\,\underset{\gamma}{\sin(\theta - \phi)}\,d\theta$$

Substituting, from trigonometry, the following relation:

$$\sin\alpha\sin\gamma = (1/2)[\cos(\alpha - \gamma) - \cos(\alpha + \gamma)]$$

then

$$\int_0^{2\pi}\sin\theta\sin(\theta - \phi)d\theta = (1/2)\int_0^{2\pi}[\cos(\theta - \theta + \phi) - \cos(\theta + \theta - \phi)]d\theta = (1/2)\int_0^{2\pi}[\cos\phi - \cos(2\theta - \phi)]d\theta$$

$$= (1/2)[\theta\cos\phi - (1/2)\sin(2\theta - \phi)]_0^{2\pi} = (1/2)[2\pi\cos\phi - (1/2)\sin(-\phi) - 0 + (1/2)\sin(-\phi)] = \pi\cos\phi$$

$$\therefore \text{drag} \sim \cos\phi.$$

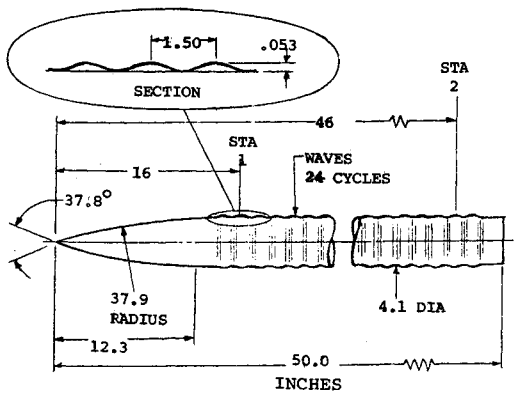

Fig. 4 Sketch of wind-tunnel model.

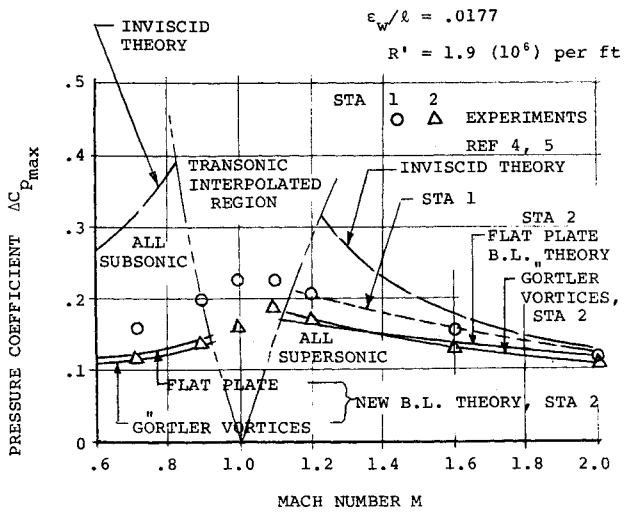

Fig. 5 Pressure coefficient vs Mach number $\sim R'$ = 1.9 (10⁶)/ft.

Substituting Eq. (23) into Eq. (24) and performing the indicated integration yields

$$\Delta C_{D_p} = (\beta/4)(\cos\phi)C_{p^2_{max}} \tag{25}$$

or

$$\Delta C_{D_p} = (\beta/4)C_{p^2_{max_i}}(\Delta C_{p_{max}}/\Delta C_{p_{max_i}})^3 = \frac{\beta}{4}\Delta C_{p^2_{max_i}}\cos^3\phi \tag{26}$$

IV. Region of Applicability—Subsonic and Supersonic Flow

The upper limit of Mach number for the subsonic theory (Sec. II) occurs when the local velocity at the wave crest becomes sonic, at a stream Mach number less than unity; and the lower limit of Mach number for the supersonic theory (Sec. III) occurs when the local velocity corresponding to maximum pressure becomes sonic, at a stream Mach number greater than unity. The limiting condition for aerodynamic analyses occurs when the local pressure ratio is 0.528, i.e., when

$$(P/P_t)_{sonic} = (1 \pm 0.7M^2\Delta C_{p_{max}})/(1 + 0.2M^2)^{3.5} = 0.528 \tag{27}$$

In Eq. (27) the term $1/(1 + 0.2M^2)^{3.5}$ is the mean pressure ratio and the term $\pm 0.7M^2\ \Delta C(p_{max})$ is the variation due to the waves. A graphic presentation of Eq. (27) for a given wave and B.L. combination shows how the flow regimes are divided into all subsonic, mixed, and supersonic (Fig. 3). In the example shown, the mixed flow region, wherein the values of pressure coefficient are interpolated between the subsonic and supersonic solutions, extends from M = 0.90 to M = 1.14.

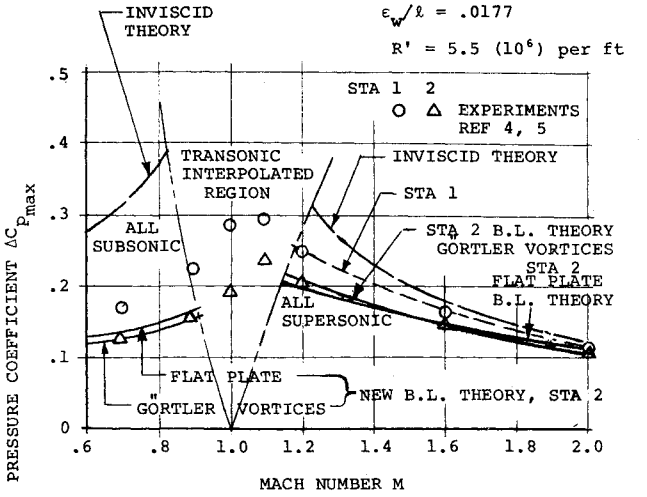

Fig. 6 Pressure coefficient vs Mach number $\sim R'$ = 5.5 (10⁶)/ft.

V. Correlation of Experiment and Theory—Pressure Coefficient and Phase Shift

A. Experiments

The experimental data used for the correlation of experiment and theory of the amplitude and phase-shift of the pressure variation due to a wavy surface are the results published in Refs. 4 and 5 for fabricated transverse waves applied to a body of revolution. The body of revolution is a 50-in. long, 4.1-in. diam, 3-caliber-nose ogive cylinder. Twenty-four waves are installed on the cylindrical part of the body, as shown in Fig. 4. The pressure of the smooth model along the cylindrical portion, except for the transonic regime, is nearly constant. The pressure coefficients on the smooth model at the test stations (x = 16 in., and x = 46 in.) are approximately $\Delta C_p = -0.01$ for M = 0.7 and M = 0.9, and approximately $\Delta C_p = +0.02$ at M = 1.2. Thus the pressure and velocities at the test stations, without the wave perturbation, are very near freestream values.

The half-height of the wave is ϵ_w = 0.0265 inches and the length of the wave is l = 1.5 in. (Fig. 4). The ratio of radius variation from the mean is 0.0265/2.05 = 1.3%. The wave parameter ϵ_w/l = 0.0265/1.5 = 0.0177 was selected as representative of fabrication imperfections found on transonic aircraft of aluminum construction. The value ϵ_w/l = 0.0177 also is representative of values measured on wrinkle patterns of wing surfaces of transonic aircraft under several g's static loading.[8]

The experiments were made in the wind tunnels at the NASA Langley Research Center and cover the Mach number range from M = 0.7 to M = 2.0. A turbulent B.L. flow was assured for all experiments by the use of a carborundum-grain trip near the tip of the model nose. Pressure measurements of the waves were made at Stations 1 and 2, from M = 0.7 to M = 2.0, at several different values of Reynolds number.

B. Analysis

The experimental data selected for analysis (at Station 2) represent a low Reynolds number, $R' \cong$ 1.9 (10⁶) per ft, and a high Reynolds number, $R' \cong$ 5.5 (10⁶) per ft. The low Reynolds number flow has a thicker boundary layer and a lower value of the amplitude of the pressure wave. The experimental data points were faired to determine the pressure peaks, and the total height of the pressure-coefficient wave was divided by two, and plotted vs Mach number in Figs. 5 and 6.

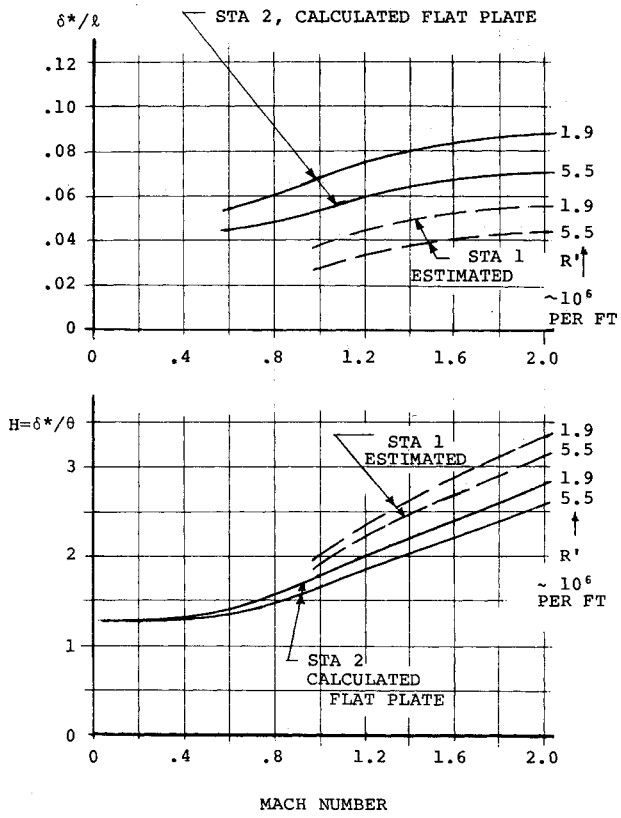

Fig. 7 B.L. characteristics: pressure coefficient analysis.

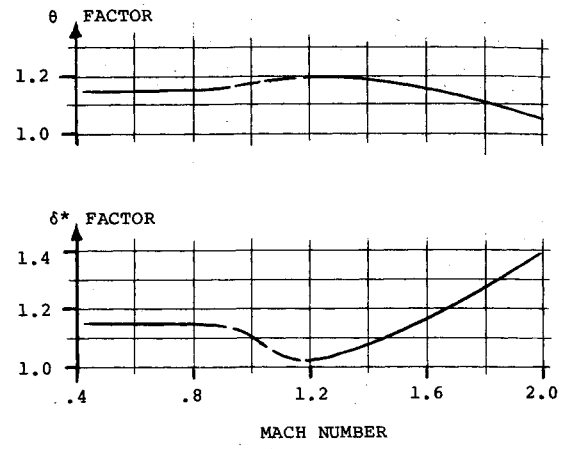

Fig. 8 Estimated B.L. modifications due to Görtler vortices: pressure correlation.

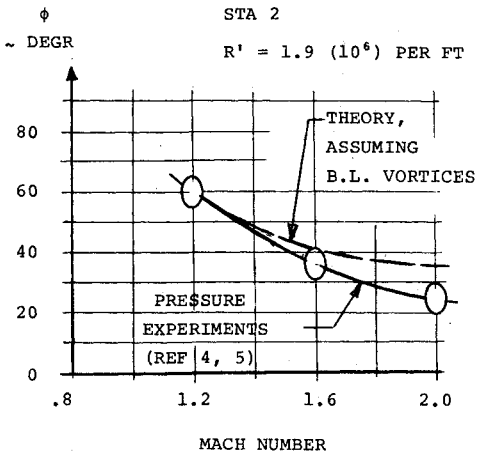

Fig. 9 Phase angle ϕ vs Mach number.

Station 2 rather than Station 1 is selected for the correlation analysis because the boundary layer developed over the length of the cylinder is closely analogous to that developed over a flat plate, providing a convenient comparison with flat-plate B.L. theory.

The pressure coefficient vs Mach number was calculated using B.L. parameters derived from flat plate theory and also using B.L. parameters modified according to the estimated effect of Görtler vortices generated by the surface waviness. The agreement between B.L. theory and experiment is quite good, much better than the agreement between inviscid flow theory and experiment (Figs. 5 and 6). Including the effect of Görtler vortices improves the correlation of theory and experiment, but the effect of the Görtler vortices does not appear to be pronounced. However, in the drag correlation the pressure coefficient term is raised to the third power, and then the effects of the Görtler vortices become important and must be included for good correlation of theory and experiment.

The flat plate boundary-layer calculations used for Station 2 are based on B.L. profiles from Ref. 7 (e.g., Fig. 21.7, pp. 546, Ref. 7). The B.L. determinations are partly analytical and partly graphical, and the analysis assumes a temperature recovery factor of 0.89. The use of flat-plate theory to correlate with experiments on a body of revolution is believed justified in this case because of the small variation in radius due to the surface wave (1.3% variation from the mean) and because the positive and negative pressure peaks are averaged. The B.L. characteristics so determined are plotted in Fig. 7. Figure 7 also shows the estimated values of B.L. characteristics at Station 1, providing agreement between theory and experiment with respect to the pressure coefficients. The data for Station 1 is not part of the correlation of experiment and theory for the pressure coefficient, but is used later in the paper (in the correlation of experiment and theory for drag) wherein the B.L. properties at Stations 1 and 2 are averaged as a baseline for the drag determination. The B.L. properties at Station 1 are quite different from those on flat plate because Station 1 is immediately aft of a region of accelerated flow (immediately aft of the nose cone).

The primary effect of the Görtler vortices generated by the waves is to increase both the B.L. momentum thickness θ and displacement thickness δ^*. The amount of B.L. thickening as a function of Mach number is determined from the drag analysis for the supersonic regime and is estimated for the subsonic regime (Fig. 8). A more comprehensive discussion of the Görtler vortices and their effect is included in the drag analysis (Sec. VI).

The aft phase shift ϕ can be measured on the data plots of Refs. 4 and 5, wherein the experimentally determined pressure wave and the theoretical inviscid flow pressure wave are superimposed on the same figure. The agreement between experiment and B.L. theory with respect to ϕ is very good at Mach 1.20, but the experimental values appear to become progressively less than the theoretical values at Mach 1.61 and 2.01 (Fig. 9). Perhaps the discrepancy at the higher Mach numbers reflects a spanwise variation of ϕ due to the pattern of the vortices.

A better correlation of experiment and theory with respect to ϕ may be that provided by the drag analysis, Sec. VI, wherein $\cos^3 \phi$ is a factor in the wave drag expression [Eq. (26)].

VI. Correlation of Experiment and Theory—Drag Coefficient

A. Introduction to the Drag Analysis

The drag model used in the correlation analysis is the same model shown in Fig. 4. Calculations of vortex

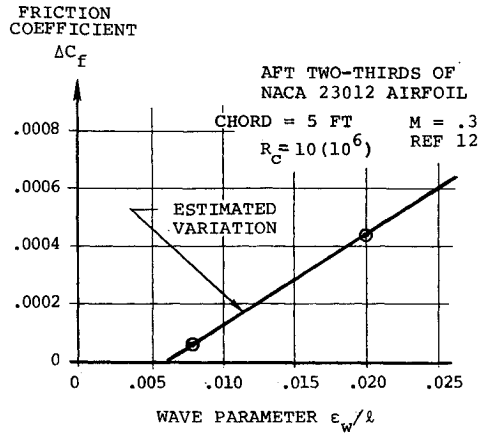

Fig. 10 Subsonic friction coefficient caused by surface waviness (Görtler vortices).

strength due to the waves, according to the methods of Smith,[9] show that a well-formed B.L. vortex system, strong enough to cause B.L. transition from laminar to turbulent flow, is generated by the first 3 waves in the supersonic flow regime. The B.L. vortices (Görtler vortices) are generated in the concave region of the waves and grow in strength with each successive wave. The Görtler vortices are described in some detail here because they have a significant effect on the drag correlation.

The Görtler vortices are stationary vortices with axes in the stream direction, and with vortex motion extending beyond the undisturbed boundary layer. An illustration of the vortices on a concave surface is presented in Fig. 17.31, pp. 442, Ref. 7. The Görtler vortices are generated in and persist in either laminar or turbulent boundary layers and in either subsonic or supersonic boundary layers. The characteristics of the Görtler vortices and the extent of concave curvature required to cause transition from laminar to turbulent flow have been determined analytically by Smith,[9] but, to the knowledge of this author, no one has published experiments or analyses to evaluate the drag associated with the vortices.

The presence of the B.L. vortices on the drag model is evidenced by the wavy boundary-layer profiles shown in Fig. 6f of Ref. 10. The wavy profiles are characteristics of Görtler vortices and are similar to profiles of B.L. vortices measured by the author in wind tunnels and on high subsonic aircraft, in connection with laminar flow B.L. research. Grid-type measurements, rather than a single profile, are required to adequately define the characteristics of the B.L. vortices; but such measurements are not available for the drag model analyzed.

Görtler vortices affect the drag determination in several ways. In both subsonic and supersonic flow the B.L. vortices increase the average surface friction, thicken the boundary layer, and modify its shape. In supersonic flow the modification of the B.L. thickness and shape can have a significant effect on the pressure drag.

The calculations and estimates with respect to the modification of friction drag and B.L. characteristics due to Görtler vortices necessarily are approximations because of the limited amount of published data on the subject and because of the limited scope of this paper. The material presented is believed to be sufficient to verify the effect of the vortices and to introduce a subject worthy of further experimental and analytical research.

B. Friction Drag Coefficient Due to Görtler Vortices

In 1939 the NACA published the results of experiments made at the Langley Memorial Aeronautical Laboratory to determine the added drag due to transverse waves on an NACA 23012 wing.[11] Wave configurations with $l = 3.0$ in. and $\epsilon_w = 0.060$ in. ($\epsilon/l = 0.020$) applied to the aft two-thirds of both surfaces of the 5 ft chord wing increased the surface friction by $\Delta C_f = 0.00044$, referred to the total area of wavy surface. The set of experiments with waves 0.4 as high showed only 0.15 as much increment in surface friction. One may assume the added drag is caused by Görtler vortices and that at some smaller wave height, the vortex strength is insufficient to affect the friction drag. If such is the case, the variation in added friction with wave height may be approximately as shown in Fig. 10.

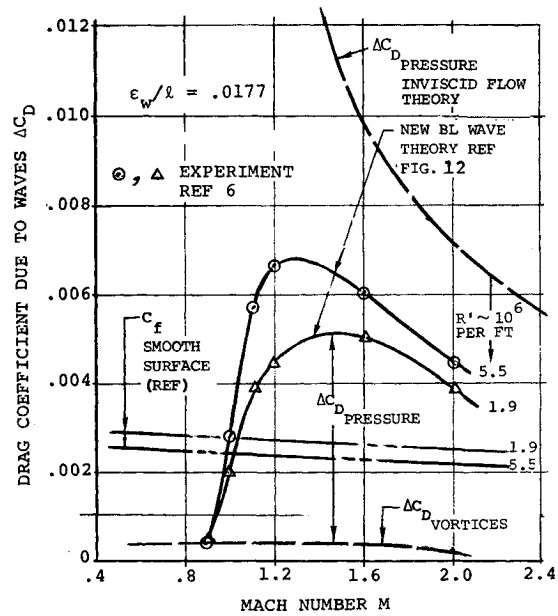

Fig. 11 Drag coefficient due to surface waves.

Drag force determinations on the body of revolution shown in Fig. 4, with waves ($\epsilon_w/l = 0.0177$) covering the cylindrical part of the body, show a drag coefficient increment at Mach 0.8 of $\Delta C_D \cong 0.0004$ at the low Reynolds number and $\Delta C_D \cong 0.0003$ at the high Reynolds number (Ref. 6, Fig. 10b).

The two experiments described indicate that the added drag coefficient due to Görtler vortices is approximately 10% to 15% of the surface friction coefficient for turbulent flow, for wave parameter value of $\epsilon_w/l = 0.02$.

C. Pressure-Drag Coefficient

The added drag of the surface waves on the model (shown in Fig. 10 of Ref. 6) is plotted in Fig. 11 for both low and high Reynolds numbers. The added drag due to the waves in supersonic flow is roughly twice the friction drag of the smooth surfaces, as indicated in Fig. 11. The theoretical drag coefficient for inviscid supersonic flow over the surface waves is much greater than the measured drag coefficient, as shown. The pressure-drag coefficient for real flow is the difference between the total added drag measured and the surface friction contribution due to Görtler vortices.

The correlation analysis for the pressure-drag coefficient calculates and analyzes the boundary-layer properties that result in the measured drag. The boundary-layer properties determined in Sec. V for Stations 1 and 2 are averaged, and then the average is modified to account for the presence of the Görtler vortices. The modification amounts to an increase in the momentum thickness θ, which is equivalent to an increase in friction drag, and a modification (increase) of the boundary-layer displacement thickness δ^* (Fig. 12). The percentage increase in momentum thickness (friction drag) required to satisfy the drag correlation analysis is approximately 20% for Mach 1.20, 15% for

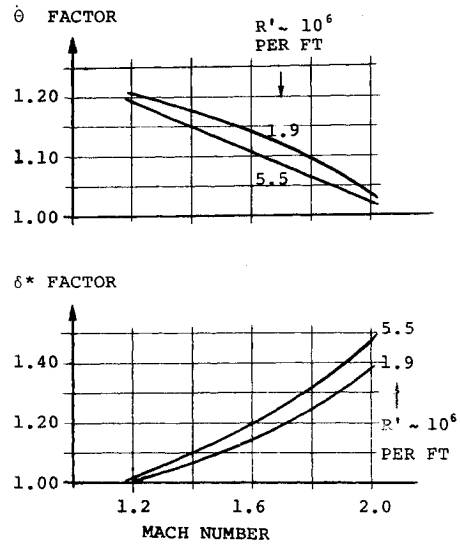

Fig. 12 B.L. modifications due to Görtler vortices: drag correlation.

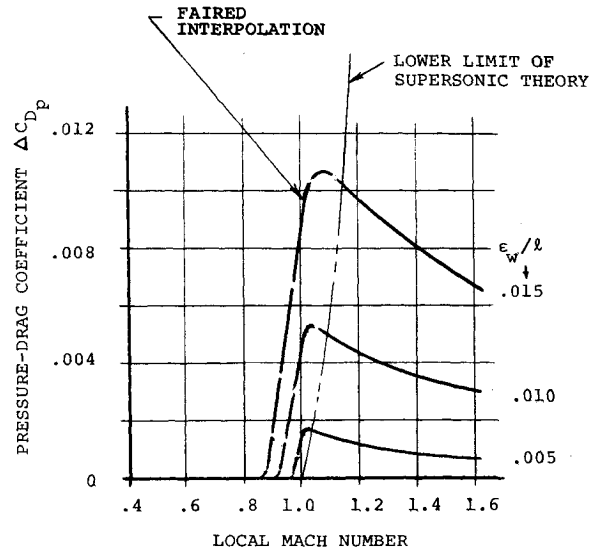

Fig. 14 Pressure-drag coefficient of surface-waves in aft part of wing. 60% to 90% chord, $\delta^*/l = 0.02$.

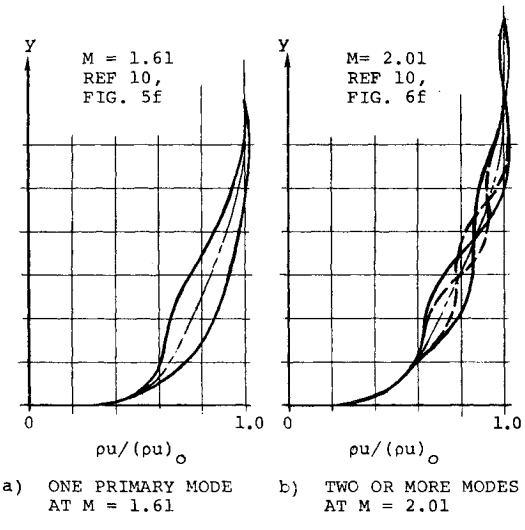

Fig. 13 B.L. profiles showing modes of Görtler vortices.

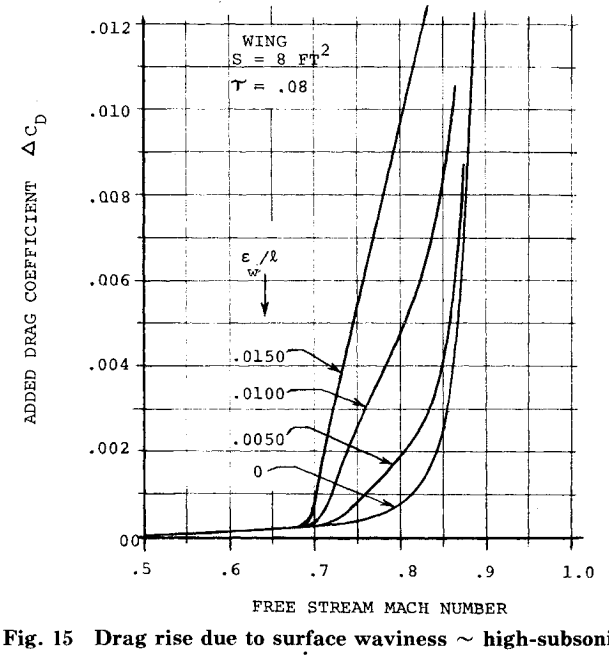

Fig. 15 Drag rise due to surface waviness ~ high-subsonic wing.

Mach 1.6, and approximately 5% for Mach 2.0, the same order of magnitude as the friction increase determined in the subsonic experiments described in Sec. VI-A. The friction increase may be less for Mach 2.0 than for Mach 1.6 because of different vortex modes. The B.L. profile measurements of Ref. 10 indicate a single vortex mode for Mach 1.61 and a multiple vortex mode for Mach 2.01 (Fig. 13). A graphic solution for the average momentum thickness of the single vortex mode at M = 1.6 (with boundary-layer profile similar to Fig. 13a) also shows approximately 15% increase over that of the undisturbed boundary layer. The graphic analysis is not included here because of limited length of the paper.

The analysis described above shows good agreement between experiment and theory if the effects of Görtler vortices are included in the estimate of B.L. properties, and poor agreement if the effects of Görtler vortices are neglected.

The importance of using the proper values of B.L. parameters in the drag analysis can be inferred from the drag coefficient equation, in which the term containing the B.L. parameters H and δ^*/l is raised to the third power [Eqs. (22) and (26)].

VII. Calculation of Subsonic Drag-Rise Caused by Wing Surface Waviness

Supersonic pressure drag due to surface waviness can be superimposed on the supersonic portions of a subsonic wing to determine the effect on the drag-rise characteristics. For each wave size investigated, a graph of pressure-drag coefficient vs Mach number is made, utilizing the method of Sec. IV to determine the beginning of the pressure-drag region and the lower limit of the supersonic region. The curves of pressure-drag coefficient are faired between the beginning Mach number and the region of all-supersonic flow (see Fig. 14, for example). The pressure-drag coefficient is used in conjunction with local Mach number distribution on the wing to determine and integrate the added drag coefficient due to the surface waviness. The analysis assumes that the particular wave size being investigated covers that portion of the wing for which the local flow is supersonic. The results of such an investigation applied to the wing of a subsonic target

drone show that the surface waviness of magnitude $\epsilon_w/l > 0.005$ has a significant detrimental effect on the drag-rise characteristics of the wing (Fig. 15). The example shown in Figs. 14 and 15 is simplified to the extent that the B.L. thickness parameter is assumed to be $\delta^*/l = 0.01$ in the forward region (accelerated flow) and $\delta^*/l = 0.02$ in the aft region (decelerated flow). The average value of δ^*/l is 0.015, which can be assumed to apply to the midchord region. The value $\delta^*/l = 0.015$ corresponds to an infinite number of combinations of Reynolds numbers and wavelength, but actually was calculated for a 1.5 ft chord wing with 1 in. long surface waves, traveling at 400 kts at sea level standard conditions. In order to simplify the analysis of this example, the effect of Görtler votices is assumed to be negligible. The results of the example show that a significant penalty to high-subsonic flight performance can result from a relatively small amplitude of surface waviness, compared with waviness commonly found on military aircraft.

Conclusions and Recommendations

The B.L. theory presented provides simple and realistic solutions for the pressure and drag due to transverse waves in subsonic and supersonic flow. The solution for the transonic regime can be made by interpolation of the solutions for the subsonic and supersonic regimes. The accuracy of the solution is dependent upon how well the B.L. properties of shape and thickness (H and δ^*) are known, but appears to be adequate for any practical aerodynamic analysis and is much better than that provided by the inviscid flow theory in the high-subsonic and low-supersonic flow regimes.

The correlation of experiment and theory as presented involves a rather extensive analysis to supplement very limited experimental measurements of the B.L. characteristics, but the correlation is considered adequate to verify the validity of the theory as an approximate soltuion. Additional pressure and B.L. measurements for the experiments analyzed are needed in order to provide a comprehensive and direct correlation of experiment and theory over the entire range of test conditions, and thereby verify the accuracy of the solutions presented.

Application of the theory to a subsonic wing shows that surface waviness of magnitude $\epsilon_w/l > 0.005$ (magnitudes commonly found on military aircraft) causes a significant detrimental effect on the drag-rise characteristics of the aircraft.

For configurations with repeated transverse surface waves, the Görtler vortices generated in the boundary layer, in both subsonic and supersonic flow apparently can have an important effect in modifying the drag characteristics.

References

[1]Ackeret, J. "Leiftkräfte and Flügel, die mit grösserer als Schallgeschwindigkeit bewegt werden," *Zeitschrift für Flugtechnik und Motorluftschiffahrt,* 16, 1925, pp 72–74. Translated in Tech. Memo. 317, 1925, NACA.

[2]Ackeret, J. "Über Luftkräfte bei sehr grossen Geschwindigkeiten insbesonders bei ebenen Strömungen," *Helvetica Physica Acta 1,* 1928, pp 301–322.

[3]Liepmann, H. W. and Roshko, A., *Elements of Gas Dynamics,* GALCIT Aeronautical Series, Wiley, New York, 1958, pp 208–215.

[4]Czarnecki, K. R. and Monta, W. J., "Pressure Distributions due to Two-Dimensional Fabrication-Type Surface Roughness on an Ogive Cylinder at Transonic Speeds," TN D-3516, Aug. 1966, NASA.

[5]Czarnecki, K. R. and Monta, W. J., "Pressure Distributions and Wave Drag due to Two-Dimensional Fabrication-Type Surface Roughness on an Ogive Cylinder at Mach Numbers of 1.61 and 2.01," TN D-835, June 1961, NASA.

[6]Czarnecki, K. R. and Monta, W. J., "Roughness Drag due to Two-Dimensional Fabrication-Type Surface Roughness on an Ogive Cylinder from Force Tests at Transonic Speeds," TN D-5004, Jan. 1969, NASA.

[7]Schlichting, H., *Boundary Layer Theory,* McGraw-Hill, New York, 1960, pp. 358, 546.

[8]Heitmeyer, J. C. and Smith W. G., "Effects of Simulated Skin Wrinkles of the Wing Surface on the Aerodynamic Characteristics of Two Wing-Body Combinations Employing Wings of Low Aspect Ratio at Subsonic and Supersonic Speeds," RM A52E23, Aug. 1952, NACA.

[9]Smith, A. M. O., "On the Growth of Taylor-Görtler Vortices along Highly Concave Walls," *Quarterly of Applied Mathematics,* Vol. XIII, No. 3, Oct. 1955, pp. 233–262.

[10]Czarnecki, K. R. and Monta, W. J., "Boundary Layer Velocity Profiles and Skin Friction due to Surface Roughness on an Ogive Cylinder at Mach Numbers of 1.61 and 2.01," TN D-2048, Dec. 1963, NASA.

[11]Hood, M. J., "The Effects of Surface Waviness and Rib Stitching on Wing Drag," TN 724, Aug. 1939, NACA.